PROSPECTS
IN PHARMACEUTICAL SCIENCES

Prospects in Pharmaceutical Sciences, -
https://prospects.wum.edu.pl/

*Original Article*

# A SCIENTIFIC EXPLORATION OF CO-AMORPHOUS FORMULATION DRIVEN BY KNOWLEDGE BASED VIRTUAL SCREENING FOR SOLUBILITY AND BIOAVAILABILITY ENHANCEMENT OF DARUNAVIR

**Ashwini Madgulkar[1], Mangesh Bhalekar[2], Abhishek Kunjir[3], Maryam Mulla*[3]**

[1] *Department of Pharmaceutics, Principal of Pharmacy College, AISSMS College of Pharmacy, 411001 Pune, India.*

[2] *Department of Pharmaceutics, Professor of Pharmaceutics, AISSMS College of Pharmacy, 411001 Pune, India.*

[3] *Department of Pharmaceutics, Student of Pharmaceutics, AISSMS College of Pharmacy, 411001 Pune, India.*

* Correspondence, e-mail: maryammulla89@gmail.com

*Received: 28.02.2025 / Revised: 07.05.2025 / Accepted: 12.05.2025 / Published online: 07.08.2025*

**ABSTRACT**

Co-amorphous systems (CAMS) have been studied as a solubility enhancement tool for the drugs facing solubility and bioavailability challenges. They have also been used to improve the stability with respect to amorphous state which is responsible for higher dissolution of the drug. This study aimed to obtain the mechanistic insights into co-amorphous formulation and improvement of the solubility of Darunavir, thereby establishing bioavailability advantage over the pure drug. To select the co-former, various virtual screening methods was employed such as the Hansen Solubility Parameter and Flory-Huggins Interaction Parameter, leading to the selection of Para-Amino Benzoic acid as a co-former. Various methods for preparation such as solvent evaporation, quench cooling and spray drying techniques were employed for co-amorphization. Based on dissolution performance the SE method was selected as it showed a 36.9-fold improvement in solubility, while dissolution studies demonstrated a 3.39-fold improvement. Dissolution studies of CAMS prepared by solvent evaporation method in 1:1 molar ratio established 1.19- and 1.25-fold better performance than 1:2 and 2:1 molar ratio, respectively. The prepared CAMS was characterized by FTIR, DSC, PXRD. Study of CAMS prepared by *ex-vivo* results demonstrated a 1.84-fold superior permeation, while *in-vivo* results confirmed a 1.72-fold improvement in oral bioavailability. Further, one-way analysis of variance (ANOVA) was applied to results of *in vitro* drug release, *ex vivo* permeation and *in vivo* pharmacokinetic study followed by Dunnett's test, which revealed that the increase in drug release, permeation and oral bioavailability of CAMS, were statistically significant at a probability level of $p < 0.05$ when compared with the pure crystalline drug darunavir.

**KEYWORDS:** Co-amorphous, Solubility enhancement, Oral bioavailability enhancement, Darunavir, Hansen Solubility Parameter.



**List of abbreviations and Symbols**

| | |
|---|---|
| CAMS | Co-amorphous Systems |
| HSP | Hansen Solubility Parameter |
| SE | Solvent Evaporation |
| QC | Quench Cooling |
| SD | Spray Drying |
| DSC | Differential Scanning Calorimetry |
| XRD | X-ray Diffraction |
| FTIR | Fourier Transform Infra Red |
| BCS | Biopharmaceutical Classification Systems |
| HIV | Human Immuno Virus |
| CYP | Cytochrome P |
| P-gp | Para – glyco Protein |
| ICH | International Conference for Harmonization |
| UV | Ultra Violet |
| Rpm | Revolutions per minute |
| HPLC | High Performance Liquid Chromatography |
| MP | Melting Point |
| RH | Relative Humidity |
| PABA | Para-Amino Benzoic acid |

## 1. Introduction

In recent years, drug discovery and development have seen significant advancements due to computational tools and virtual screening-based software leading to an exponential increase in the throughput of new chemical entities. While virtual screening tools enable the development of highly specific and selective molecules, they also come with downsides. These molecules tend to have inherently high molecular weights and higher partition coefficients, leading to formulation issues such as low solubility and/or poor permeability. Consequently, these novel molecules often fall into BCS (Biopharmaceutics Classification System) classes II, III, or IV, limiting their absorption and bioavailability [1].

Given that over 60% of available formulations are administered orally, enhnacing solubility is a critical aspect of drug development [2]. Various strategies, including particle size reduction, salt formation, co-solvation, co-crystal preparation, solid dispersion approaches, and formulation techniques like microspheres, niosomal and liposomal preparations, have been explored to achieve this. However, these approaches often encounter drawbacks such as increased dosage requirements, stability challenges, lengthy preparation methods, and lower drug loading capacities. One promising strategy to address the solubility issues involves converting crystalline drug form into their amorphous counterparts. Amorphous drugs exhibit higher apparent solubility and dissolution profiles compared to their crystalline counterparts [3]. Co-amorphous systems (CAMS) offer a suitable mechanism for drug amorphization. These systems have shown promise in enhancing the solubility of BCS class II and IV drugs. Unlike solid dispersions that use polymeric materials, CAMS systems employ low molecular weight excipients (such as drugs, amino acids or organic acids) as a co-formers [4,5].

CAMS are defined by stabilization of amorphous drug molecule with the help of co-former (binary CAMS) or co-formers (ternary CAMS) thereby forming a single homogenous system [6], referred to as glassy systems or glassy solutions. Advantages of CAMS over other techniques include improved solubility [7,8], improved dissolution profile [7,9], higher drug loading capacity [6,9,10,12], higher stability [9,11], multiple drug therapy [9], lowering of hygroscopicity of drug [12].

Amorphous materials pose a stability challenge due to their lower stability as compared to their crystalline counterparts. Conversely, crystalline forms exhibit reduced solubility and limited bioavailability. Addressing both solubility and stability is crucial. Co-amorphous systems (CAMS) capitalize on the benefit of both crystalline and amorphous drug properties, including improved physical stability and enhanced solubility and dissolution profiles [13,14].

Darunavir, is an antiretroviral selective protease inhibitor drug from the second-generation class used in HIV treatment. Darunavir is administered alongside Ritonavir in combination thearpy for HIV treatment. Single-drug pharmacokinetics reveal a bioavailability of approximately 37% [15]. The limited bioavailability may be attributed to Darunavir's metabolism by CYP3 enzymes and P-gp efflux [16,17]. Additionally, Darunavir's reported solubility of around 0.15 Kg/$m^3$ underscores the need for solubility enhancement [18].

The absorption of darunavir is noatbly influenced by food intake, with enhanced bioavailability observed when administered with meals, particularly those containing fat.(lembo ref 19). This food effect is attributed to increased drug solubility and enhanced lymphatic transport, leading to improved systemic exposure. Once absorbed, darunavir undergoes extensive binding to plasma proteins, primarily albumin and alpha-1 acid glycoproetin, limiting its free fraction available for antiviral activity. The distribution of darunavir into various tissues and body fluids is still under investigation, but it is believed to penetrate well into lymphoid tissues, which serve as mahor reservoirs for HIV. Darunavir's metabolism is primarily mediated by the cytochrome P450 enzyme system, specifically CYP3A4, in the liver.(20) this metabolic pathway can be affected by other medications taken at the same time, causing drug interactions [21]. Furthermore, darunavir is often co-administered with ritonavir, a potent CYP3A4 inhibitor, to boost its plasma concentrations and prolong its half-life, thereby enhancing its antiviral efficacy [22].

The pharmacodynamic of darunavir revolve around its potent inhibition of the HIV-1 protease, an enzyme crucial for viral maturation and replication. By selectively binding to the protease active site, darunavir prevents the cleavage of viral pluproteins into functional proteins, leading to the production of immature, non-infectious viral particles [23].

Developing a co-amorphous system of Darunavir with various co-formers aims to improve the solubilty, subsequent bioavailability, and stability of Darunavir.

## 2. Materials and Methods

### 2.1. Materials Collection

Mylan Laboratories Limited, India, kindly provided a gift sample of Darunavir ethanolate. Para-amino benzoic acid, methanol, potassium dihydrogen phosphate, disodium hydrogen phosphate, hydrochloric acid, acetonitrile, and other required chemicals were procured from LOBA CHEMIE Pvt. Ltd, India.

### 2.2. Co-former selection based on solubility parameter [11]

Solubility parameter (δ) quantifies a system's cohesive qualities by taking the square root of its cohesive energy density. Hansen solubility parameter (HSP) model was given in 1967 to predict the miscibility between two components. It states that components with similar δ or closer δ values would be miscible with one another [19,20].

HSP is denoted as δ and derived by the equation [21,22]:

$$\Delta\delta^2 = \delta d^2 + \delta p^2 + \delta h^2$$

The group contribution method is used to compute these Hansen 3-dimensional solubility parameters as:

$$\delta d = \frac{\Sigma Fdi}{\Sigma Vi}$$

$$\delta p = \frac{\sqrt{F2pi}}{\Sigma Vi}$$

$$\delta h2 = \frac{\Sigma Ehi}{\Sigma Vi}$$

Where, *Fd*, *Fp*, and *Eh* are group contributions to the

dispersion forces, polar interaction, and hydrogen bonding, respectively. *Vi* is the molar volume of groups.

Dispersion forces (δd), polar forces (δp) and hydrogen bonding forces (δh) are the three partial solubility parameters in HSP [21,22]. The components are miscible with one another if the HSP difference between two components is less than 7 $Mpa^{0.5}$ [21,22]. More the miscibility of the two components better is the co-formability of the co-former. The calculations of HSP values were done by Fedors Group Contribution method [23,24]. The co-former with lowest difference between the HSP values of drug and co-former was selected as the suitable co-former. Calculation by Fedors Group Contribution method involves complete breakdown of the chemical entity of the chemicals under study at its functional groups level followed by assigning the total number to each functional group level followed by assigning the total number to each functional group after which the total forces i.e. summation of δd, δp, δh is done based on assigned values of these forces for each functional group [25,26]. From the HSP values obtained Para-Amino Benzoic acid was chosen as a co-former of interest.

### 2.3. Co-former selection based on Flory-Huggins Interaction Parameter [20,26]

Miscibility of two molecules can also be predicted by Flory Huggins Interaction parameter, according to which two components are miscible when x≠0. Good miscibility is predicted by a negative or slightly positive value of x, whereas immiscibility/non-miscibility is indicated by a high positive number [6,27,28].

Flory Huggins Interaction parameter was calculated virtually by Amsterdam Modelling Suite software i.e. COSMOS-RS program. FastSigma was used to estimate the sigma profile of the compounds. After optimization of the compounds COSMOS-SAC method followed by 2013 – ADF Xiong parameter was used to investigate FHI parameter.

According to FHI Parameter Para-Amino Benzoic acid was chosen as the co-former.

### 2.4. Co-former selection based on Docking Studies [29,30]

Docking studies reveal the potential interactions between the drug and co-former. The interactions indicate bonds that may be formed during co-amorphization process. The glide score and docking score are indicative of the interactions between the drug and co-former. More negative the docking and glide score better is the interaction, thus better is the co-formability of the co-former. Thus, the co-former with highest negative energy was chosen as the co-former.

Molecular docking was performed with software Maestro Schrodinger. Maestro's protein preparation wizard created the drug structure, and LigPrep 2.3 wizard created the co-former structure. The drug structure was optimized by OPLS force field.

After ligand preparation for drug and co-formers, grid generation was performed in which the docking of molecule was achieved. According to docking studies Para-Amino Benzoic acid with -3.834 glide score was chosen as co-former.

Co-former Para-Amino Benzoic acid was selected based on the agreement between all the three selection parameters.

### 2.5. Drug – Co-former Compatibility Studies [6,36]

The potential chemical interaction between the drug and co-formers were screened using FT-IR analysis. Equimolar amount of drug and co-former were accurately weighed and mixed thoroughly. This physical mixture along with pure drug and co-former were separately stored in stoppered glass vials at 40°C for two weeks. After the study period the samples were analyzed by FT-IR for any chemical interactions between the drug and co-former.

### 2.6. Preparation of Darunavir Co-amorphous system by Solvent Evaporation Method

After precisely weighing Darunavir and Para-amino benzoic acid in a 1:1 molar ratio, they were dissolved independently in methanol. The above solutions were subjected to ultrasonication for 15 minutes at 25°C in ultrasonic bath – USB025 at frequency 40 KHz. The solutions were mixed thoroughly and subjected to evaporation. The product thus obtained was scraped, collected and air dried for 24 hours, passed through sieve 100 µm and stored in desiccator for further evaluation. The advantages of SE method are useful for thermosensitive drugs; more uniform dispersion of the drug and co-former and disadvantage are organic solvents are used and proper evaporation of solvent not occurred may be leads to recrystallization of drug [7].

### 2.7. Preparation of Darunavir Co-amorphous system by Quench Cooling Method

Darunavir and Para-Amino Benzoic acid were precisely weighed in a 1:1 molar ratio, homogeneously mixed and the physical mixture was then heated to the temperature just above melting point of higher melting component. The melt thus obtained was quickly quench cooled with liquid nitrogen. The resultant mass thus obtained was scrapped, collected and passed through sieve 100 µm for uniform particle size distribution and kept in desiccator for additional analysis. Advantages of quench cooling methods are rapid formation of CAMS and disadvantages are may be degradation of drug due to heat and which may result in phase separation [31].

### 2.8. Preparation of Darunavir Co-amorphous system by Spray Drying Method

The solution of Darunavir and Para-Amino Benzoic acid in 1:1 molar ratio was prepared in methanol. The solution was filtered and sprayed into a hot air stream in spray dryer where spherical, narrow size distributed CAM particles of Darunavir with Para-amino benzoic acid were obtained. The inlet and outlet temperature were kept at 30°C and 45°C, respectively with the spray rate of 2 ml/min. The product thus formed by spray drying was scrapped and collected (Labultima). Thermal exposure during spray drying was kept below the $T_g$ of the system formed to avoid crystallization of Darunavir. The product obtained was stored in desiccator for further evaluation. The advantages of spray drying method are more uniform CAMS formed, useful for thermosensitive drugs and disadvantages are may be thermal degradation occur due to heat due to high inlet and outlet temperature [32,33].

### 2.9. Drug content determination

A volumetric flask was filled with precisely weighed CAMS equivalent to 10 mg, which was then dissolved in methanol. The resulting solution was filtered through a 0.45 µ membrane filter after being diluted with methanol to a volume of 10 ml. Following the proper dilutions, the drug concentration of the sample was ascertained by UV analysis at a wavelength of 263 nm [6,34].

### 2.10. Solubility studies

Solubility determination of Darunavir and CAMS was carried out by shake flask method [35]. Excess amount of drug was transferred to conical flask which contain 50 ml of distilled water. These flasks were subjected to orbital shaking and maintained at 50 rpm at 37 ± 1°C. Following 24 hours period, a sample was taken out of the flask, centrifuged for 15 minutes at 3500 rpm, and the supernatant was separated. This supernatant was appropriately filtered, diluted and solubility of drug and co-amorphous system was determined by UV analysis at 263 nm wavelength.

### 2.11. Powder X-ray Photo Diffraction Analysis [6,9,10]

The powdered samples of Darunavir, Para-amino benzoic acid and CAMS were analyzed for XRD patterns using an X-ray diffractometer (Bruker D2 Phaser). The PXRD analysis was employed for characterizing the solid-state characteristics of drug and co-amorphous system. Copper rod was used as a source for generation of x-rays at voltage and current range of 40 KV and 40 mA, respectively. At a wavelength of 2.28970 A° and a diffraction angle of 2θ the C-ray diffraction was established. The scan speed was kept at 10,000 degrees per minute and scan step time was set at 0.8 seconds.

### 2.12. Fourier Transform Infrared Spectroscopy (FT-IR) Analysis [6,36]

Fourier transform infrared spectroscopy (FT-IR) was evaluated using FT-IR spectrometer (FTIR-4600 type A series ATR Pro One). Pure drug, physical mixture and CAMS infrared spectra were all obtained in triplicate spanning a 4000 – 400 $cm^{-1}$ range (32 scans, resolution of 4 $cm^{-1}$). These graphs were analyzed for any chemical interactions along with any addition or absence of peaks corresponding to the functional group in the pure drug samples and the CAMS formulation.

### 2.13. Thermal Analysis [6,37]

Thermal analysis of Darunavir and CAMS was subjected to differential scanning calorimetry using (HITACHI DSC V7020) instrument. 2 mg sample, was transferred into aluminum pans, sealed, and heated to an isothermal temperature between 30-300 °C at a regulated rate of 10 °C per minute in a nitrogen-maintained environment with a flow rate of 60 ml/minute. The DSC thermograms which was obtained used to study the possible interactions, confirm the amorphization process, predict the $T_g$ of the samples and other possible interaction occurring within the samples. The enthalpy and melting point were analyzed by standard analysis tool.

### 2.14. Prediction of Glass Transition temperature by using Gordon Taylor Equation [38,39]

The $T_g$ for the system is considered as a point where a slight but a noticeable downward trend starts to occur in a thermogram followed by sharp rise in the graph or restoration in the thermogram. This observed glass transition temperature can be compared with theoretical values of glass transition temperature predicted via Gordon Taylor equation which is stated as:

$$Tg1,2 = \frac{w1tg1 + Kw2Tg2}{w1 + Kw2}$$

Where, $T_{g1,2}$ is the glass transition temperature of the respective binary system, $T_{g1}$ and $T_{g2}$ are the $T_g$ values of the two amorphous components in the system and $w_1$ and $w_2$ are the weight fractions of these components, respectively. The constant K is calculated by:

$$K = \frac{Tg1\,.\,\rho1}{Tg2\,.\,\rho2}$$

Where, the powder densities of the two amorphous components, 1 and 2, are denoted by $\rho_1$ and $\rho_2$ 5respectively.

### 2.15. Physical Stability Studies [39,40]

Amorphous drugs tend to crystallize over a period. Thus, this tendency of CAM formulation to crystallize during storage was studied using stability chamber (REMI CHM-6S) at 40 ± 2 °C at 75 ± 5% RH. These samples before and after storage for 3 months were subjected to DSC analysis to observe changes if any occurred during the storage.

### 2.16. *In Vitro* Release studies [6,9,41]

Using a USP II paddle apparatus dissolution equipment (ELECTROLAB INSPIRE 08), the *in vitro* dissolution of the Darunavir (600 mg) and CAMS equivalent to a single dose (600 mg) was carried out in triplicate. The control group used in in-vitro test was a pure drug (600 mg). A temperature of 37 ± 0.5°C and a paddle rotation speed of 50 rpm was used to carry out the dissolution process using 900 ml of the dissolution medium at 37 ± 0.5 °C (simulated gastric media pH 1.2, Phosphate buffer pH 6.8 and distilled water). Sampling was done at the predetermined time intervals (10, 20, 30, 40, 50 and 60 minutes), where 5 ml of sample was withdrawn, filtered using 0.45 µm syringe filter. Following each sampling, an equal volume dissolution medium was replenished. The samples were then analyzed using UV spectrophotometry at 263 nm after appropriate dilutions. Cumulative amount of drug dissolved was calculated.

### 2.17. *Ex vivo* Permeation Study [42,43]

Using an everted rat intestine model, the permeability of CAMS (equivalent to 600 mg) and pure darunavir drug (Control) (600 mg) across the rat gut was assessed. About 8-9 cm of rat intestinal segment was isolated and washed with Krebs Ringer solution. Both ends were mounted on the assembly and the ends were tied with the help of thread, from the other open end of assembly 10 ml of phosphate buffer pH 6.8 was filled using a syringe. The prepared model was suspended in the dissolution apparatus thereby allowing measurement of drug release and simultaneous permeation of the drug across the intestinal sac. Sampling was done at 10, 20, 30, 40, 50 and 60 minutes, respectively. The amount of drug permeated was estimated using UV spectrophotometry.

### 2.18. *In Vivo* Pharmacokinetic Study [6,10,44]

*In vivo* pharmacokinetic investigation was performed on Male Wistar rats. These rats were housed in a room with a 12 hours dark/light cycle, 25 ± 2 °C and relative humidity of 55 ± 5%. Following at least two weeks of adaptive feeding, 18 rats (n=6) were split into three groups at random. Before dose administration these rats were kept on a fasting for a period of 12 hours.

Group 1: Darunavir suspension (Control)

Group 2: Physical mixture of Darunavir and Para-Amino Benzoic acid suspension

Group 3: CAMS suspension

The suspensions were fed to the animals in respective group with the aid of oral feeding needle (Dose – 10 mg/kg).

Retro-orbital punctures were used to obtain 0.5 ml blood samples, which were then placed into centrifuge tubes containing heparinized sodium at 0.5-, 0.75-, 1-, 2-, 3-, 4-, 6-, 8-, 12-, 24-, 48- and 72-hours following treatment. All blood samples were centrifuged for 15 minutes at 10,000 rpm followed by complete protein precipitation by addition of organic solvent (acetonitrile). These samples were then centrifuged for 15 minutes at 10,000 rpm, and the resulting plasma, or supernatant, was used for further analysis by HPLC.

Maximum plasma concentration (Cmax), the time to reach the maximum plasma concentration (Tmax), and the total area under the plasma concentration-time curve ($AUC_{0\rightarrow t}$ and $AUC_{0\rightarrow\infty}$) were determined. The plasma drug concentration time profiles were plotted from the analyzed samples.

### 2.19. Moisture Uptake and Residual Organic Content Analysis [45]

To assess moisture uptake Samples of Darunavir, CAMS prepared by SE, QC and SD were weighed and placed in pan of moisture balance of moisture analyzer (Mettler Toledo). The temperature was set at 50 °C for 10 minutes. After switching 'ON' the machine, the digitized readings of moisture and organic solvent loss as a percentage of solvent evaporated from the sample were recorded after the specific time interval (10 minutes).

### 2.20. Micromeritic Study [46,47]

The flow properties of Darunavir and CAMS were evaluated by bulk density, tapped density, Carr's Index, Hausner's ratio and angle of repose.

### 2.21. Statistical Analysis

One-way analysis of variance (ANOVA) followed by Dunnett's test was employed for the analysis of in vitro drug release, ex vivo permeation and pharmacokinetic studies. At probability level < 5 % ($p < 0.05$), results were considered significant. This was performed using GraphPad Prism 10 (GraphPad Software, Inc., La Jolla, CA, USA) software.

## 3. Results

### 3.1. Co-former selection based on Hansen Solubility Parameter

Solubility parameter (δ) quantifies a system's cohesive qualities by taking the square root of its cohesive energy density. Hildebrand proposed Hansen solubility parameter (HSP) model to predict the miscibility between two components [48]. According to it components with similar δ or approximately close δ would be miscible with one another [19,20]. The components with HSP difference less than 7 $(Mpa)^{0.5}$ are considered to be miscible with one another, as the co-formability of co-former depends on miscibility with drug [21,22].

The values of hydrogen bonding forces, dispersion forces and polar forces derived from the structure of Darunavir and Para-Amino Benzoic acid are fairly similar that is less difference between them (Table 1), hence they form a good drug co-former pair from chosen co-formers. Due to bulky nature of Darunavir the polar forces in the molecule are almost negligible, while the amino group and carboxylic group in amino benzoic acid being on the opposite end of the benzene ring negate each other's polar force thus reducing the polar forces within the molecule. Contrastingly with other co-formers i.e. tartaric acid, fumaric acid, succinic acid, maleic acid and adipic acid the more difference in the HSP value is dictated mainly due to increase in the COOH groups and absence of any counter functional groups in their structure which contribute to increase in hydrogen bonding forces and increased polar forces thereby increasing the difference from the δ value of darunavir. The increase in ionizable groups (majorly COOH) within these co-formers are responsible for increasing the dispersion forces within these co-formers overall increasing the difference from the δ value of darunavir, thereby indicating the increase in immiscibility between the drug- co-former pair.

The increasing order of miscibility was found to be:

Para-Amino Benzoic acid > Adipic acid > Succinic acid > Fumaric acid > Tartaric acid > Maleic acid

HSP suggest Para-Amino Benzoic acid to have better co-formability with Darunavir.

**Table 1.** Hansen Solubility Parameter values calculated by Fedor's Group Contribution Approach

| Name | δh | δd | δp | δ | Difference |
|---|---|---|---|---|---|
| **Darunavir** | 11.6789 | 19.85 | 3.3322 | 23.277 | NA |
| **Para-Amino Benzoic acid** | 12.4294 | 18.80 | 3.6453 | 22.83 | 0.447 |
| **Tartaric acid** | 28.28 | 21.86 | 12.31 | 37.81 | 14.533 |
| **Fumaric acid** | 19.06 | 17.62 | 4.8926 | 22.34 | 0.937 |
| **Succinic acid** | 14.973 | 17.937 | 4.893 | 22.34 | 0.937 |
| **Maleic acid** | 19.06 | 33.81 | 10.799 | 40.29 | 17.063 |
| **Adipic acid** | 12. | 17.62 | 4.892 | 22.34 | 0.937 |

### 3.2. Co-former selection based on Flory Huggins's Interaction Parameter

Similar to HSP model, Flory Huggins Interaction parameter is also based on the thermodynamic properties of the molecule [49]. This parameter is widely used to study the miscibility between the polymeric materials but can also be applied to other components as well. As per thermodynamics systems mutual co-existence is dependent on minimization of Gibbs free energy [50].

Flory Huggin's Interaction parameter indicates that Para-Amino Benzoic acid and Darunavir pair requires minimal Gibbs Free energy for mixing. In contrast the bulky structures of adipic acid, tartaric acid and succinic acid restricts the molecular movement thereby increasing Gibbs Free energy and larger size decreases the chances of molecular mixing thereby showing a non-favorable Flory Huggins Interaction value.

The order of miscibility between drug and co-formers as suggested by Flory Huggins Interaction Parameter was found to be:

Para-Amino Benzoic acid > Adipic acid > Maleic acid > Fumaric acid > Succinic acid > tartaric acid (Table 2)

Flory Huggins Interaction Parameter suggest Para-Amino Benzoic acid to have superior miscibility with Darunavir.

**Table 2.** Flory Huggins Interaction Parameter values obtained from AMS modelling suite

| Drug | Co-former | FHI value |
|---|---|---|
| **Darunavir** | Para-Amino Benzoic acid | -0.00584 |
| **Darunavir** | Tartaric acid | 0.00 |
| **Darunavir** | Fumaric acid | -0.00264 |
| **Darunavir** | Succinic acid | -0.00144 |
| **Darunavir** | Maleic acid | -0.00265 |
| **Darunavir** | Adipic acid | -0.0037 |

### 3.3. Co-former selection based on docking studies

The interactions revealed by docking include hydrogen bonding, pi-pi stacking, ionic interaction, etc. More negative the docking and glide score better is the interaction which suggest greater affinity between the drug molecule and the co-former selected and thus better co-formability of the co-former.

Drug- co-former docking generally involves two types of interactions viz. hydrogen bonding interaction, which is a weak bond necessary for temporary bond formation which is a prerequisite for CAMS formulations and pi-pi stacking, which contributes towards the stability of system formed. Thus, in the docked structure it is observed that darunavir and Para-Amino Benzoic acid show hydrogen bond as well as pi-pi stacking which thereby increases the binding affinity between the molecules, as opposed to other co-formers i.e. Fumaric acid, Citric acid, adipic acid, tartaric acid, maleic acid and succinic acid where hydrogen bond is the only driving force behind CAMS formulation (Table 3).

The docked structure of Darunavir and Para-Amino Benzoic acid reveal pi-pi stacking between the benzene ring of amino benzoic acid and the terminal benzene ring attached to sulphonyl group and having amine group at its terminal position there by showing better pi-pi interaction due to attachment of 2 functional groups. On the other hand, a strong hydrogen bond exists between the terminal amino group of co-former and secondary amine in the darunavir moiety which in turn is responsible for a higher negative docking score [51,52].

The binding affinity as suggested by docking studies is as follows:

Para-Amino Benzoic acid > Succinic acid > tartaric acid > Adipic acid > Fumaric acid > Maleic acid

**Table 3.** Glide score and type of interaction between drug and co-former as revealed by docking studies

| Drug | Co-former | Glide Score | Type of Interaction |
|---|---|---|---|
| **Darunavir** | Para-Amino Benzoic acid | -3.834 | Hydrogen bond and pi-pi stacking |
| **Darunavir** | Tartaric acid | -2.727 | Hydrogen bond |
| **Darunavir** | Fumaric acid | -1.621 | Hydrogen bond |
| **Darunavir** | Succinic acid | -3.157 | Hydrogen bond |
| **Darunavir** | Maleic acid | -1.621 | Hydrogen bond |
| **Darunavir** | Adipic Acid | -1.895 | Hydrogen bond |

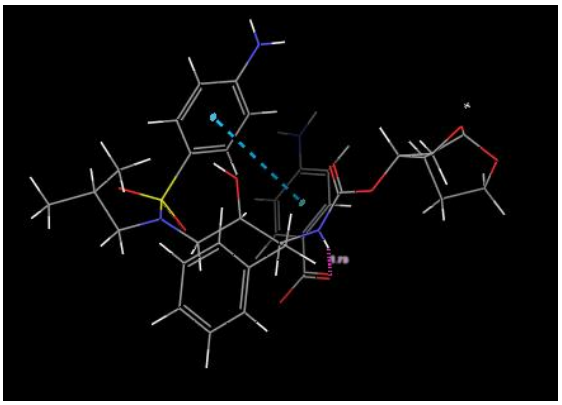

**Fig 1.** The docking image between Darunavir and Para-Amino Benzoic acid

### 3.6. Drug co-former compatibility study [6,36]

The characteristic peaks of Darunavir in its pure form indicating C-O-C stretch (1249 $^{cm-1}$), C=C stretch ($^{1446\ cm-1}$), C-O stretch (3458 $^{cm-1}$), H stretch (3307 $^{cm-1}$) and $NH_2$ stretch (3358 $^{cm-1}$) were observed (Fig 2.). Other peaks for C-C, C-H, C=C at their respective wavenumbers were also identified. Similarly, IR peaks of Para-Amino Benzoic acid at (3051 $^{cm-1}$) -OH stretch, (1660-2000 $^{cm-1}$) aromatic benzene ring stretch and (1633 $^{cm-1}$) C=O stretch (reduction in wavenumber due to conjugation) were identified (Fig 3.). The IR spectra of physical mixture

show little to no change in peaks of Darunavir appearing at 1288 $^{cm-1}$, 1440 $^{cm-1}$, 3460 $^{cm-1}$ and 3363 $^{cm-1}$ respectively, with little to no change in the wavenumber for their respective groups indicating absence of interaction between the drug and co-former. Similarly, peaks of (3059 $^{cm-1}$) -OH stretch, (1660-2000 $^{cm-1}$) aromatic benzene ring stretch and (1600 $^{cm-1}$) C=O stretch (lower intensity as compared to pure para-amino benzoic acid) of the co-former can be identified in the spectra of physical mixture thereby indicating retention of co-former thereby further asserting that there is no any interaction between the drug and co-former (Fig 4.). Thus, it can be confirmed that drug and co-former are compatible with each other.

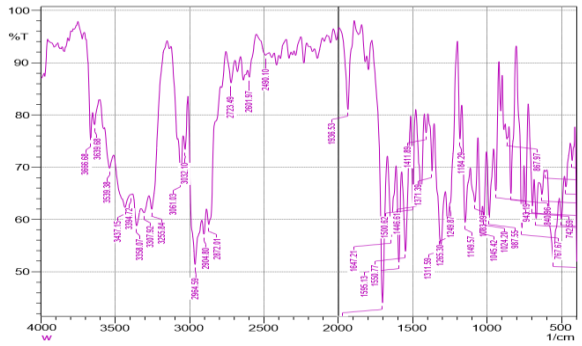


**Fig 2.** IR Spectra of Pure Darunavir

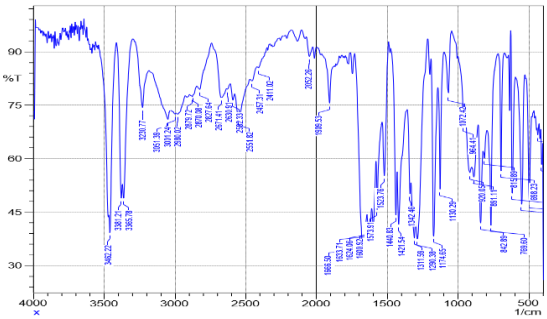


**Fig 3.** IR Spectra of Para-Amino Benzoic acid

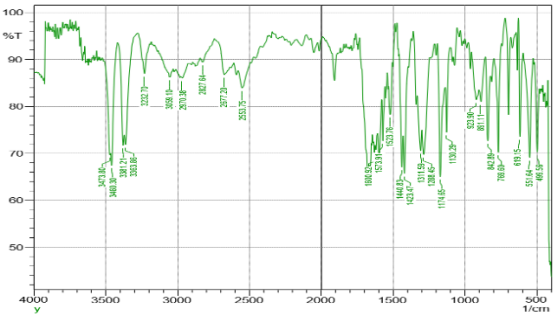


**Fig 4.** IR Spectra of physical mixture of Darunavir and Para-Amino Benzoic acid

### 3.4. Drug content determination [6,34]

The yield of CAMS prepared was maximum by solvent evaporation followed by quench cooling, while least yield was obtained by spray drying method. The low yield from spray drying was due to material adhering to the walls of cyclone separator and the connector tubing. The low drug content for quench cooling and spray drying CAMS was due to the degradation of certain portion of drug subjected to temperature above the melting point of drug. When evaluated for drug content of CAMS prepared by solvent evaporation, spray drying and quench cooling was found to be 83.3%, 77.6% and 75.8%, respectively.

### 3.5. Solubility Study [53]

To establish a net solubility advantage of CAMS over the pure form of drug, solubility experiment of the drug and its CAMS was done in distilled water. Pure drug showed 0.232 mg/ml solubility which was close to the reported value i.e. 0.15 mg/ml [18], while CAMS prepared by different methods showed exceptionally high solubility i.e. 8.562 mg/ml, 6.277 mg/ml and 6.404 mg/ml by solvent evaporation, spray drying and quench cooling method, respectively. The increment in solubility was due to the amorphization of drug present in the CAMS.The comparative decrease in solubility of CAMS by spray drying and quench cooling was due to the degradation of drug due to the heat. It was observed that the solubility of CAMS is comparatively higher than its pure form which was due to the disordered arrangement of drug molecule in the co-amorphous system which enables the solvent molecules to easily enter within matrix of the system and increase the contact space thereby increasing the solubility of the drug in its co-amorphous form. Through thermodynamic point of view the increase in solubility was attributed to the amorphous nature of the CAM system which requires less energy for the breakdown of lattice of the molecule as compared to its pure form. Higher solubility of CAMS could also be attributed to "Spring and Parachute" [54,55,56,57,58] effect which is a characteristic of CAMS, spring effect leads to generation of a metastable supersaturated state which is characterized by higher burst release of drug from the system, which could be seen by higher solubility values of Darunavir from its CAMS as opposed to its pure form.

**Table 4.** Solubility studies of Darunavir and CAMS in water

| Name | Solubility (mg/ml) |
|---|---|
| **Darunavir** | 0.232 ± 0.011 |
| **CAMS (SE)** | 8.526 ± 0.121 |
| **CAMS (SD)** | 6.277 ± 0.039 |
| **CAMS (QC)** | 6.404 ± 0.088 |
| **Reported solubility of the Darunavir** | 0.15 |

### 3.6. Powder X-ray diffraction analysis [6,9,10]

Darunavir powder subjected to XRD shows high intensity peak of the diffractogram ranging in the intensity from 780 to 8915, while 8915 being the highest intensity peak. Most of the intense peaks were observed between 15 to 25 degrees 2θ angle (Fig 5.). A total of 16 highly resolved peaks were observed throughout the whole diffractogram while a larger number (almost double) of small and less resolved peaks were also observed. Para-Amino Benzoic acid showed few highly resolved peaks ranging in the intensity from 617 to 39778. The observed peaks were highly resolved and well separated. A total of 20 highly resolved peaks were observed in which most of the peaks were of intensity less than 10000 (Fig 6.). CAMS shows a hallow diffractogram comprising of few peaks with low

intensity (Fig 7.) The presence of halo pattern which is a characteristic of amorphous material along with the presence of individual small unresolved peaks could lead to conclusion that a homogeneous system of drug and co-former was formed after co-amorphization process. The appearance of intense individual peaks for crystalline materials is due to the presence of crystalline faces of the molecule which results into diffraction of X-rays, in contrast to co-amorphous system where due to the absence of any crystal faces of the molecule the appearnace of a halo pattern is detected [59].

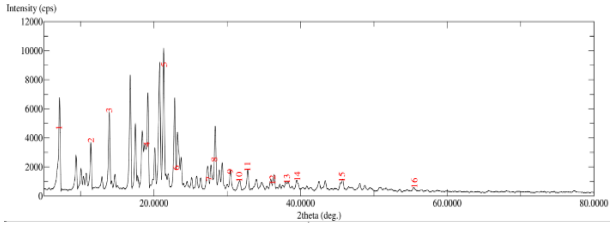


**Fig 5.** XRD diffractogram of pure Darunavir

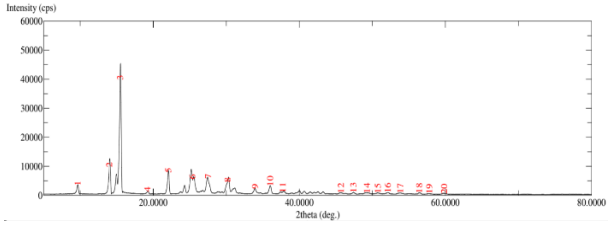


**Fig 6.** XRD diffractogram of Para-Amino Benzoic acid

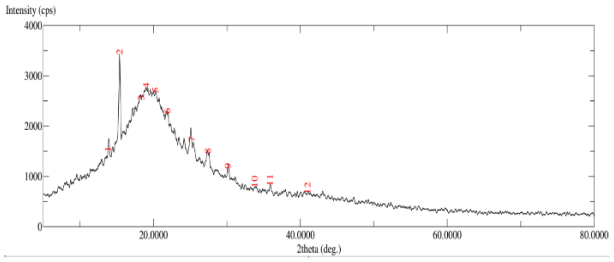


**Fig 7.** XRD diffractogram of CAMS

### 3.7. Fourier Transform Infrared Spectroscopy (FT-IR) Analysis [6,36]

FT-IR analysis was performed to detect any structural changes that may have occurred in the drug during the co-amorphization process that may hinder the kinetics and dynamics of the drug when given in CAM system.

Samples of Darunavir and CAMS were analyzed for any changes in characteristic peaks corresponding to the drug molecule. The characteristic peaks of darunavir showing C-O-C stretch (1249 $^{cm-1}$), C=C stretch (1446 $^{cm-1}$), C-O stretch (3458 $^{cm-1}$), H stretch (3307 $^{cm-1}$), and $NH_2$ stretch (3358 $^{cm-1}$) were observed (Fig 8.). Similar peaks of C-O-C stretch (1247 $^{cm-1}$), C=C stretch (1446 $^{cm-1}$), C-O stretch (3456 $^{cm-1}$), H stretch (3300 $^{cm-1}$), and $NH_2$ stretch (3363 $^{cm-1}$) were observed in the IR spectra of CAMS (Fig 9.). The trivial shift in the wavenumber could be due to conjugation effect or shift due to solvent interaction. It can be inferred that the chemical integrity of the drug molecule in the CAMS is maintained despite undergoing amorphization with a co-former with the help of solvent system. Other inferential parameter supporting the above conclusion could be the appearance of IR peaks corresponding to the co-former which is an indicative of the structural integrity of co-former as well i.e. peaks at (3059 $^{cm-1}$) -OH stretch, (1660-2000 $^{cm-1}$) aromatic benzene ring stretch and (1627 $^{cm-1}$) C=O stretch (reduction in wavenumber due to conjugation) were observed with shift in wavenumber similar to that of the drug molecule. Thus, it can be inferred from the IR interpretation that SE method prepared a proper co-amorphized system of Darunavir and Para-Amino Benzoic acid without affecting the chemical and structural properties of drug and co-former.

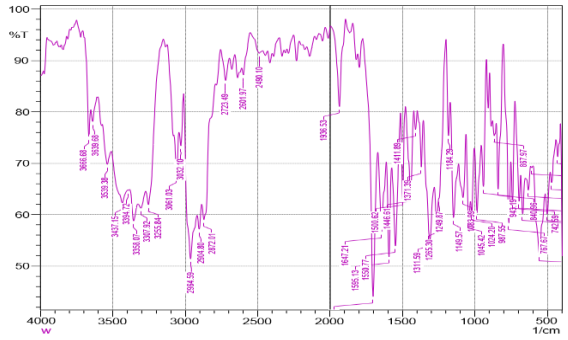


**Fig 8.** IR Spectra of Darunavir

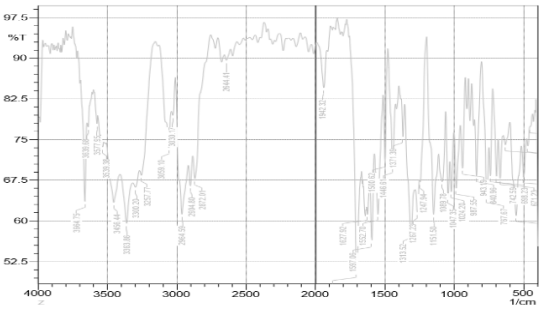


**Fig 9.** IR Spectra of CAMS

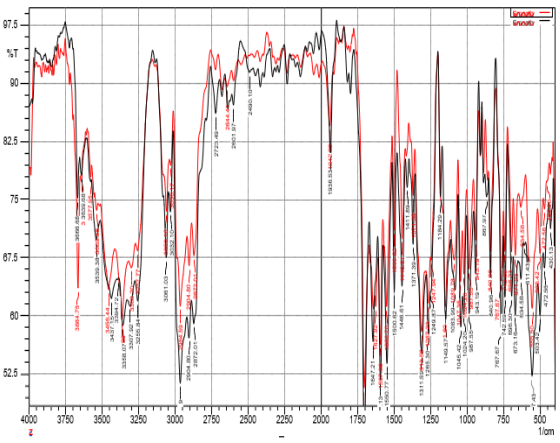


**Fig 10.** Overlay of IR Spectra of Darunavir and CAMS

### 3.8. Thermal Analysis [6,37,60]

SE, QC, and SD produced differential scanning calorimetry (DSC) thermograms for pure drug and CAMS generated in a 1:1 molar ratio. For pure drug Darunavir a sharp endothermic peak was observed at 76.9 °C (Fig 11.) indicating its sharp melting point. This sharp endotherm is an indicative of crystalline nature of the drug with a fusion enthalpy of 112 mJ m /mg. The non-existence of

any other peak in the thermogram explained the absence of any other impurity in the material as well as hydrate or solvate molecules associated with darunavir. The DSC thermogram of CAMS shows a sharp endothermic peak at 73.1 °C (Fig 12.) which is less than the pure drug which indicates that Para-Amino Benzoic acid is incorporated in the drug molecules which depresses the melting point of the pure drug. The appearance of a broad endotherm starting from 190°C and extending till 270°C further infers the incorporation of co-former within the system. The increase in fusion enthalpy from 112 to 239 mJ/mg indicates change in the crystal lattice structure i.e. addition of co-former in the drug lattice. This distorts the arrangement of the drug molecules thereby preventing the formation of crystalline structure of drug. The increase in enthalpy for melting point of drug is due to higher melting point of co-former which has additive effect on the enthalpy of the CAMS formed by solvent evaporation method. The DSC thermogram of CAMS by SD and QC shows a broad endothermic peak which is a clear characteristic of CAMS which starts from 70°C and extends till 120°C, which includes the $T_g$ of the system which was predicted by Gordon Taylor equation (Fig 13.). The presence of a broad spectrum starting from 190° to 270°C confirms the presence of co-former in the system similar to SE CAMS.

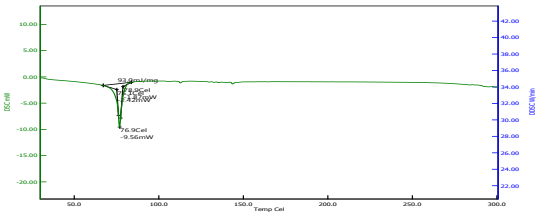


**Fig 11.** DSC thermogram of pure Darunavir

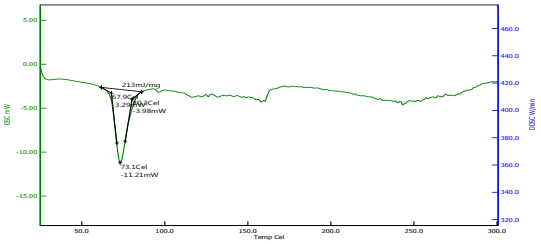


**Fig 12.** DSC thermogram of CAMS prepared by SE method

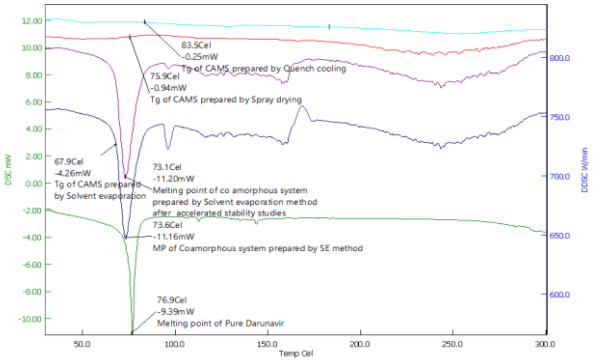


**Fig 13.** Overlay of DSC thermogram of darunavir (green), CAMS prepared by SE method kept under stability studies (Blue), CAMS prepared by SE (Purple), CAMS prepared by SD (Red), CAMS prepared by QC (Light Blue)

### 3.9. Prediction of Glass transition temperature by Gordon Taylor Equation [11,38,39,61]

Both positive and negative deviations from predicted Gordon Taylor equation are indicative of improper mixing or improper miscibility between the components but practically smaller deviations are tolerated. Non-ideal free volume additivity, component molecule interactions, and hydrogen bonding loss during mixing are some of the factors that contribute to the non-ideal mixing [62,63], which leads to negative deviations from the predicted $T_g$ values.

CAMS prepared by SE method show least deviation from predicted $T_g$ values when compared to QC and SD CAMS (Table 5.). Thus, CAMS prepared by SE method with lowest deviation from Gordon Taylor equation are expected to show better stability over time.

**Table 5.** Predicted and experimental $T_g$ values predicted by Gordon Taylor equation

| Name | Darunavir | CAMS (SE) | CAMS (SD) | CAMS (QC) |
|---|---|---|---|---|
| **Predicted $T_g$** | NA | 67.17 | 67.17 | 67.17 |
| **Experimental $T_g$** | 76.9 (Melting Point) | 67.9 | 75.9 | 83.5 |
| **Difference between predicted and experimental $T_g$** | NA | -0.73 | -8.73 | -16.33 |

### 3.10. Physical stability evaluation [39,40]

Stability of CAMS was evaluated by DSC after subjecting the samples to accelerated stability conditions for 1.2 and 3 months at 40 ± 2°C and 70 ± 5 % RH which showed comparatively less enthalpy than samples at room temperature (Fig 12,14). The appearance of a short endothermic peak near about 100°C is due to loss of water molecules which was attributed to uptake of moisture by CAMS upon exposure to accelerated conditions. The stability of CAMS could also be attributed to the formation of homodimers which form small chained like structures which is neither in crystalline form nor in amorphous form. Thus, these formed homodimers consisting of a monomer of drug and a co-former improves stability which can be explained by the fact that, for crystallization of pure drug to occur the drug should be readily available to form along chain which is prevented by monodimer [64]. For crystallization of drug to occur the drug must free itself from its dimer state, then rearrange its molecular structure and then organize itself in its crystalline form. This whole process uses considerable amount of energy; thus, the molecules tend to remain in this co-amorphous form for a considerable period.

Dissolution studies of CAMS before and after accelerated stability conditions indicate little to no effect on release of drug from CAMS (Fig 15.). Before subjecting to stress conditions, the drug release after 60 minutes was 78% while after stressed conditions it was found to be 73% which is not significant enough to indicate the decrease in release rate from CAMS after accelerated conditions

thereby indicating the physical stability of CAMS.

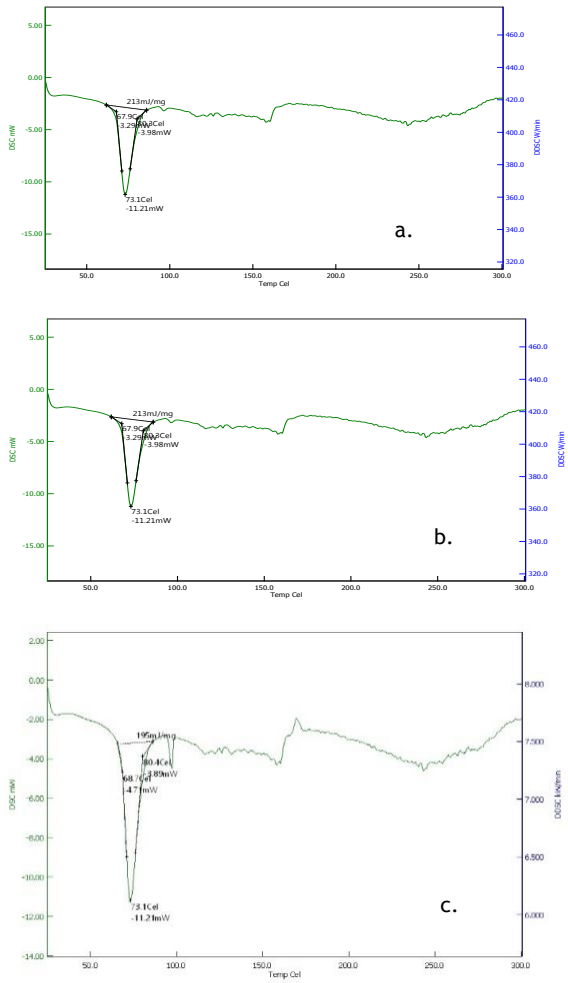


**Fig 14.** DSC thermogram of a. CAMS at 1-month b. CAMS at 2-month c. CAMS at 3-months

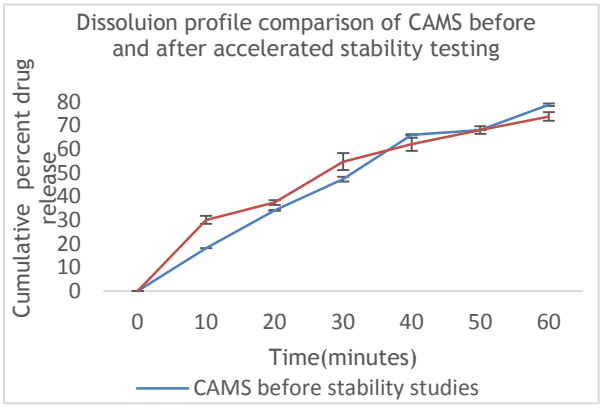


**Fig 15.** Dissolution profile comparison of CAMS before and after accelerated stability testing

### 3.11. *In-vitro* drug release study [6,9,41]

Through the dissolution profiles it was observed that pure drug darunavir (control) showed a release of 24%. Meanwhile, SE CAMS showed an impressive 79% drug release, while QC CAMS and SE CAMS showed 65.7% and 66.4% release respectively, indicating the superiority of CAMS over pure drug (Fig 15.). Thus, SE was chosen as the optimum method of preparation as it showed 3 times more dissolution as compared to pure drug and 13% more release than QC and SD method.

To study the influence of molar ratio on the drug release, CAMS were prepared in 1:1, 1:2 and 2:1 molar ratio by solvent evaporation method. It was observed that CAMS with 1:1 molar ratio show maximum release i.e. 78.8% followed by 1:2 (66.44%) and 2:1 (63%) (Fig 15.).

Due to the drug's pH-dependent solubility, dissolution test was carried in water, PBS (pH 6.8) and 0.1 N HCl to investigate how pH affects the drug release. It is evident that drug release in water as a dissolution medium is lowest i.e. 48.6% while HCl showed 84.5% release and 79% release in PBS medium (Fig 16.). Comparative high dissolution in HCl could be due to ionization caused by HCl thereby improving the dissolution rate of drug. But 6% increment in dissolution is not significant enough to derive the conclusion that there is pH dependent drug release from CAMS further proving the pH independent release characteristic of CAMS.

Further, the in vitro drug release results were analyzed using one-way ANOVA followed by Dunnett's test, which revealed that the increase in drug release of CAMS were statistically significant at a probability level of $p < 0.05$ when compared with the pure crystalline drug darunavir.

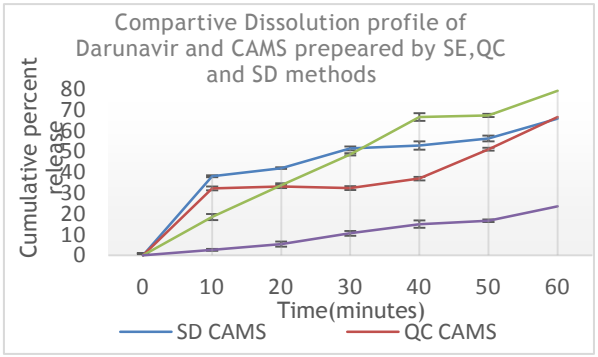


**Fig 16.** Comparative dissolution profile of Darunavir and CAMS prepared by SE, QC and SD methods

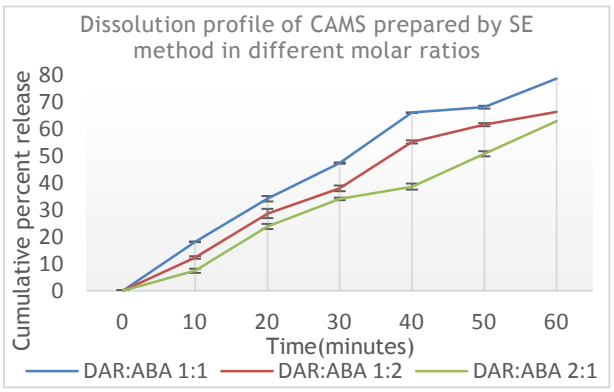


**Fig 17.** Dissolution profile of CAMS prepared by SE method in molar ratios 1:1, 1:2 and 2:1

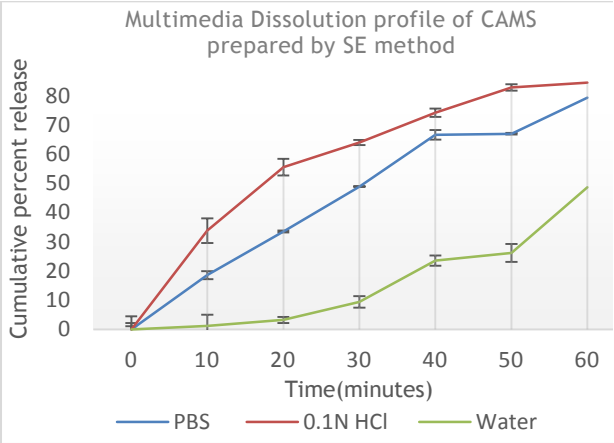


**Fig 18.** Dissolution profile of CAMS of 1:1 molar ratio in water, PBS (pH 6.8) and 0.1 N HCl

### 3.12. *Ex-vivo* permeation study

For pure darunavir the permeation across the intestinal wall was found to be 19.91% while CAMS permeation was found to be 35.6% (Fig 19.) which is 1.78 times better permeation as compared to the pure drug. The increase in permeability is owed to higher drug release from CAMS thereby achieving higher degree of solubility due to which the rate of passive diffusion across the intestinal lining seems to be elevated. This could suggest that absorption of drug through CAMS would be comparatively higher thus the bioavailability of drug would be significantly enhanced.

Further, the ex vivo drug permeation results were analyzed using one-way ANOVA followed by Dunnett's test, which revealed that the increase in drug release of CAMS was statistically significant at a probability level of $p < 0.05$ when compared with the pure crystalline drug darunavir.

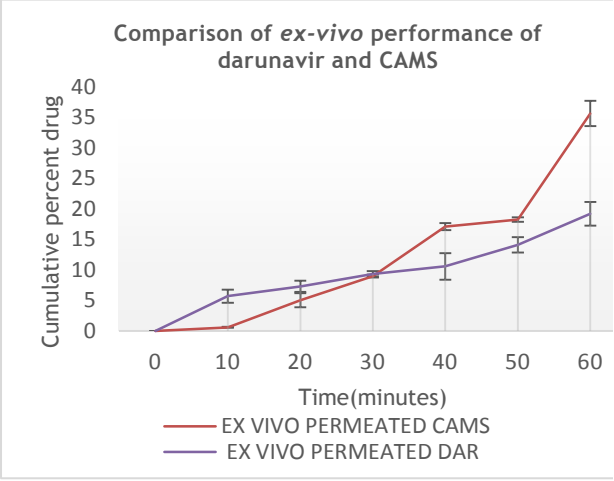


**Fig 19.** Comparison of *ex vivo* performance of darunavir and CAMS across everted rat intestine

### 3.13. *In-vivo* Pharmacokinetic Study [6,10,44]

The CAMS, Physical mixture and pure drug (control) were evaluated for *in vivo* study. Various pharmacokinetic parameters were derived from the plasma concentration time profile i.e. $t_{max}$, $C_{max}$, AUC, etc. Thus, it was observed that $t_{max}$ for pure drug darunavir and CAMS is 4 hours, and $C_{max}$ for pure drug darunavir was found to be 2.23 µg while for CAMS it was 4.33 µg (Table 6.). Thus, it can be interpretated that CAMS because of their solubility advantage exhibit better pharmacokinetic parameters as compared to the pure drug. The major difference in the *in vivo* profiles can be seen in the initial burst increase in plasma drug concentration of CAMS due to initial burst release from CAMS explained by "SPRING and PARACHUTE" effect (Fig 20.). This high release leads to greater $C_{max}$ of CAMS compared to the pure drug. After achieving maximum concentration in the plasma for both pure drug and CAMS the decrease in the concentration of drug counterparts follows linear first order elimination kinetics. The higher $C_{max}$ and AUC for CAMS are indicative of superiority of CAMS performance *in vivo* thereby, establishing its bioavailability advantage.

The *in vitro* dissolution from CAMS showed 3.39-fold improvement, subsequently *ex vivo* permeation was 1.84-fold more and in vivo study showed 1.94- and 2.2-fold improvement in $C_{max}$ and AUC, respectively. The subsequently higher improvement in ex vivo and invivo studies can be justified by the fact that conformer PABA is PgP inhibitor and DRV is a substrate for PgP efflux[65].

Further, the in vivo drug plasma concentration results were analyzed using one-way ANOVA followed by Dunnett's test, which revealed that the increase in drug release of CAMS were statistically significant at a probability level of $p < 0.05$ when compared with the pure crystalline drug darunavir.

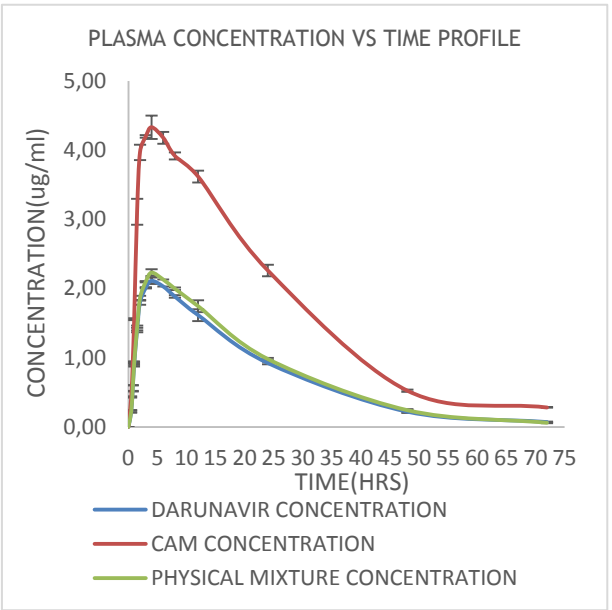


**Fig 20.** Plasma concentration vs Time profile of Darunavir, CAM and Physical mixture

**Table 6.** Comparison of Pharmacokinetic parameters of Darunavir, CAM and Physical mixture

| Sr No | Parameter | Darunavir | Physical mixture | CAMS |
|---|---|---|---|---|
| 1. | $C_{max}$ (µg/ml) | 2.23 | 2.11 | 4.33 |
| 2. | $t_{max}$ (h) | 4.00 | 4.00 | 4.00 |
| 3. | AUC $_{0-72}$ (ug.hr/ml) | 57.0626 | 56.24 | 125.694 |
| 4. | AUC $_{0-\infty}$ | 58.973 | 57.68 | 132.2 |

| | (ug.hr/ml) | | | |
|---|---|---|---|---|
| 5. | Ke ($h^{-1}$) | 0.04531 | 0.054 | 0.04376 |
| 6. | $T_{1/2}$ (h) | 15.294 | 12.833 | 15.836 |

### 3.14. Moisture uptake and residual organic content analysis [45]

Pure drug powder shows 25.49% moisture content which could be due to absorption of atmospheric moisture. CAMS prepared by SE and SD showed more amount of residual content as compared to the CAMS prepared by QC method due to trapped solvent methanol which was used in the preparation method.

**Table 7.** Moisture uptake and residual organic content analysis

| Name | Residual content (%) |
|---|---|
| **Darunavir** | 25.49 ± 0.17 |
| **CAMS SE** | 1.35 ± 0.02 |
| **CAMS QC** | 0.17 ± 0.05 |
| **CAMS SD** | 0.55 ± 0.11 |

### 3.15. Micromeritic study evaluation [46,47]

Flow property of the powdered samples was evaluated to check the flowability of samples during processing to maintain dose uniformity and weight uniformity in processed tablets. For every parameter studied CAMS showed better performance compared to pure Darunavir.

**Table 8.** Flow property comparison of pure drug and CAMS powder

| Property | Darunavir | CAMS |
|---|---|---|
| **Bulk Density** | 0.591 | 0.5714 |
| **Tapped Density** | 0.666 | 0.625 |
| **Angle of Repose** | 50.19° (Poor) | 29.3° (Excellent) |
| **Hausner's Ratio** | 1.35 (Poor) | 1.093 (Excellent) |
| **Carr's Index** | 28.34 (Poor) | 9.38 (Excellent) |

## 4. Discussion

In this study, CAMS in anticipation to achieve improved solubility, dissolution and thereby improved permeability were successfully prepared by SE, SD and QC method. SE method showed best solubility and dissolution due to the uniform molecular dispersion of the drug and co-former. Characterization test were performed by thermal analysis, FT-IR analysis and XRD analysis after preparation of CAMS which indicated the formation of co-amorphous system of Darunavir with Para-Amino Benzoic acid as a co-former. Thermal analysis of CAMS showed positive deviation of calculated value of glass transition revealed single homogenous system formation and also improved stability of CAMS under stressed conditions. FT-IR study revealed that there is no chemical interactions or structural changes in CAMS system thereby maintaining the molecular integrity of the drug. The XRD analysis results showed that the absence of sharp peaks in CAMS system which means the crystaline drug changed into the amorphous state.

Solubility studies and multi-media dissolution studies concluded superiority of CAMS over pure darunavir, while *ex-vivo* studies and *in-vivo* studies indicated the improvement of permeability and thus bioavailability of CAMS. Stability studies and dissolution studies of CAMS under accelerated stability condition concluded the stability of CAMS for long period. These studies revealed the potential of Para-Amino Benzoic acid in formation of co-amorphized form of Darunavir and improved performance over pure form of Darunavir.

## 5. Conclusion

The CAMS prepared by SE method has showed a 37-fold solubility increase, 3.39-fold improvement in *in vitro* dissolution and a 1.84-fold increase in *ex vivo* permeation compared to pure darunavir. *In vivo* studies showed an 1.94-fold improvement in Cmax and a 2.2-fold increase in AUC, indicating significantly enhanced bioavailability. Therefore, from the findings it can be concluded that the co-amorphization through solvent evaporation method improved the solubility and oral bioavailability of darunavir significantly.

The limitations of the study include long-term stability study. The stability studies were only performed for 3 months under accelerated conditions. A longer-term stability assessment would be valuable to evaluate the physical stability of the co-amorphous system over extended periods.

The future study include to conduct long-term stability studies (e.g. 6 months, 1 year) under various storage conditions to thoroughly assess the physical stability of the darunavir-para-amino benzoic acid co-amorphous system.

**Author Contributions:** Conceptualization, Dr. Ashwini Madgulkar. and Dr. Mangesh Bhalekar; methodology, Dr. Mangesh Bhalekar. and Abhishek Kunjir; validation, Abhishek Kunjir. and Maryam Mulla; Investigation, Abhishek Kunjir; resources, Dr. Mangesh Bhalekar; data curation, Abhishek Kunjir; writing-original draft preparation, Abhishek Kunjir. and Maryam Mulla; visualization, Maryam Mulla; supervision, Dr. Mangesh Bhalekar and Abhishek Kunjir; project administration, Dr. Ashwini Madgulkar. and Dr. Mangesh Bhalekar. All authors have read and agreed to the published version of the manuscript.

**Funding**: This research received no external funding.

**Informed Consent Statement**: Not relevant

**Conflicts of Interest**: The authors declare no conflict of interest.

## References

1. Hauss, D.J. Oral lipid-based formulations. *Adv. Drug. Deliv. Rev.* **2007**, *59(7)*, 667-676. DOI: 10.1016/j.addr.2007.05.006.
2. Alqahtani, M.S.; Kazi, M.; Alsenaidy, M.A.; Ahmad, M.Z. Advances in oral drug delivery. Front Pharmacol. **2021,** 12, 618411. DOI: 10.3389/fphar.2021.618411.
3. Zhang, J.; Guo, M.; Luo, M.; Cai, T. Advances in the development of amorphous solid dispersions: The role of polymeric carriers. Asian J Pharm Sci. 2023, 18(4),

100834. DOI: 10.1016/j.ajps.2023.100834.

4. Forster, A.; Hempenstall, J.; rades, T. Characterization of glass solutions of poorly water-soluble drugs produced by melt extrusion with hydrophilic amorphous polymers. J Pharm Pharmacol. 2001, 53(3), 303-15. DOI: 10.1211/0022357011775532.
5. Vasconcelos, T.; Sarmento, B.; Costa, P. Solid dispersions as strategy to improve oral bioavailability of poor water soluble drugs. Drug Discov Today. 2007, 12(23-24), 1068-75. DOI: 10.1016/j.drudis.2007.09.005.
6. Liu, J.; Grohganz, H.; Lobmann, K.; Rades, T.; Hempel N.J. Co-amorphous drug formulations in numbers: Recent advances in co-amorphous druf formulations with focus on co-formability, molar ratio, preparation methods, physical stability, in vitro and in vivo performance, and new formulation strategies. Pharmaceutics. 2021, 13(3), 389. DOI: 10.3390/pharmaceutics13030389.
7. Yamamura, S.; Gotoh, H.; Sakamoto, Y.; Momose, Y. Physicochemical properties of amorphous precipitates of cimetidine-indomethacin binary system. Eur J Pharm Biopharm. 2000, 49(3), 259-65. DOI: 10.1016/s0939-6411(00)00060-6.
8. Turek, M.; Rozycka-Sokolowska, E.; Koprowski, M.; Marciniak, B.; Balczewski, P. Role of hydrogen bond in formation of co-amorphous valsartan/nicotinamide composition of high solubility and durability with anti-hypertension and anti-COVID-19 potential. Mol Pharmaceut. 2021, 18(5), 1970-84. DOI: 10.1021/acs.molpharmaceut.0c01096.
9. Alleso, M.; Chieng, N.; Rehder, S.; Rantanen, J.; Rades, T.; Aaltonen, J. Enhanced dissolution rate and synchronized release of drugs in binary systems through formulation: Amorphous naproxen-cimetidine mixtures prepared by mechanical activation. J Control Release. 2009, 136(1), 45-53. DOI: 10.1016/j.jconrel.2009.01.027.
10. Shayanfar, A.; Ghavimi, H.; Hamishekar, H.; Jouyban, A. Coamorphous atorvastatin calcium to improve its physicochemical and pharmacokinetic properties. J Pharm Sci. 2013, 16(4), 577-57. DOI: 10.18433/j3xs4s.
11. Yarlagadda, D.L.; Anand, V.K.; Nair, A.R.; Sree, K.N.; Dengale, S.J.; Bhat, K. Considerations for the selection of co-formers in the preparation of co-amorphous formulations. Int J Pharm. 2021, 602, 120649. DOI: 10.1016/j.ijpharm.2021.120649.
12. Karagianni, A.; Kachrimanis, K.; Nikolakakis, J. Co-amorphous solid dispersions for solubility and absorption improvement of drugs: Composition, preparation, characterization and formulations for oral delivery. Pharmaceutics. 2018, 10(3), 98. DOI: 10.3390/pharmaceutics 10030098.
13. Hancock, B.C.; Zografi, G.; Characteristics and significance of the amorphous state in pharmaceutical systems. J Pharm Sci. 1997, 86(1), 1-12. DOI: 10.1021/js9601896.
14. Kaushal, A.M.; Gupta, P.; Bansal, A.K. Amorphous drug delivery systems: molecular aspects, design, and performance. Crit Rev Ther Drug Carrier Syst. 2004, 21(3), 133-93. DOI: 10.1615/critrevtherdrugcarriersyst. v21.i3.10.
15. Dierynck, I.; De Wit, M.; Gustin, E.; Keuleers, I.; Vandersmissen, J.; Hallenberger, S.; Hertogs, K. Binding kinetics of darunavir to human immunodeficiency virus type 1 protease explain the potent antiviral activity and high genetic barrier. J Virol. 2007, 81(24), 13845-51. DOI: 10.1128/JVI.01184-07. Epub 2007 Oct 10.
16. Fujimoto, H.; Higuchi, M.; Watanabe, H.; Koh, Y.; Ghosh, A.K.; Mitsuya, H.; Tanoue, N.; Hamada, A.; Saito, H. P-glycoprotein mediates efflux transport of darunavir in human intestinal Caco-2 and ABCB1 gene-transfected renal LLC-PK1 cell lines. Biological and Pharmaceutical Bulletin. 2009, 32(9), 1588-93. DOI: 10.1248/bpb.32.1588.
17. Back, D.; Sekar, V.; Hoetelmans, R. M. Darunavir: pharmacokinetics and drug interactions, Antivir Ther. 2008, 13(1), 1-13. DOI: 10.1177/135965350801300101.
18. Darwish, I.A.; Al-Majed, A.A.; Alsaif, N.A.; Bakheit, A.H.; Herqash, R.N.; Alzaid, A. Darunavir: A comprehensive profile. Profiles Drug Subst Excip Relat Methodol. 2021, 46, 1-50. DOI: 10.1016/bs.podrm.2020.07.001.
19. Deng, Y.; Liu, S.; Jiang, Y.; Martins, I.C.; Rades, T. recent advances in co-former screening and formation prediction of multicomponent solid forms of low molecular weight drugs. Pharmaceutics. 2023, 15(9), 2174. DOI: 10.3390/pharmaceutics15092174.
20. Deng, Y.; Luo, W.; Zheng, Z.; Wei, G.; Liu, S.; Jiang, Y.; Yang, H. Predication of co-amorphous formation using non-bonded interaction energy: Molecular dynamic simulation and experimental validation. Chemical Engineering Science. 2023, 272, 118618. DOI: 10.1016/j.ces.2023.118618.
21. Feng, Y.; Li, B.; Yang, L.; Liu, Y. Co-amorphous delivery systems based on curcumin and hydroxycinnamic acids: Stabilization, solubilization, and controlled release. LWT. 2022, 170, 114091. DOI: 10.1016/j.lwt.2022.114091.
22. Deng, Y.; Deng, W.; Huang, W.; Zheng, Z.; Zhang, R.; Liu, S.; Jiang, Y. Norfloxacin co-amorphous salt system: Effects of molecular descriptors on the formation and physical stability of co-amorphous systems. Chemical Engineering Science. 2022, 253, 117549. DOI: 10.1016/j.ces.2022.117549.
23. Gani, R. Group contribution-based property estimation methods: advances and perspectives. Current Opinion in Chemical Engineering. 2019, 23, 184-96. DOI: 10.1016/j.coche.2019.04.007.
24. Vay, K.; Scheler, S.; Friess, W. Application of Hansen solubility parameters for understanding and prediction of drug distribution in microspheres. Int J Pharm. 2011, 416(1), 202-9. DOI: 10.1016/j.ijpharm.2011.06.047.
25. Tsutsumi, S.; Kato, Y.; Namba, K.; Yamamoto, H. Functional composite material design using Hansen solubility parameters. Results in Materials. 2019, 4, 100046. DOI: 10.1016/j.rinma.2019.100046.
26. Mark, J. Physical properties of polymers, 3rd edition.; Cambridge University Peak, Cambridge, 2004; pp. 72-144.
27. Thakral, S.; Thakral, N.K. Prediction of drug-polymer

miscibility through the use of solubility parameter-based Flory-Huggin's interaction parameter and the experimental validation: PEG as model polymer. J Pharm Sci. 2013, 102(7), 2254-63. DOI: 10.1002/jps.23583.

28. Shi, Q.; Moinuddin, S.M.; Cai, T. Advances in coamorphous drug delivery systems. Acta Pharm Sci B. 2019, 9(1), 19-35. DOI: 10.1016/j.apsb.2018.08.002.

29. Garbiec, E.; Rosiak, N.; Tykarsha, E.; Zalewski, P.; Cielecka-Piontek, J. Sinapic acid Co-amorphous systems with amino acids for improved solubility and antioxidant activity. Int J Mol Sci. 2023, 24(6), 5533. DOI: 10.3390/ijms24065533.

30. Lobmann, K.; Laitinen, R.; Grohganz, H.; Gordon, K.C.; Strachan, C.; Rades, T. Coamorphous drug systems: enhanced physical stability and dissolution rate of indomethacin and naproxen. Mol Pharm. 2011, 8(5), 1919-28. DOI: 10.1021/mp2002973.

31. Lobmann, K.; Laitinen, R.; Grohganz, H.; Gordon, K.C.; Strachan, C.; Rades, T. Coamorphous drug systems: enhanced physical stability and dissolution rate of indomethacin and naproxen. Mol Pharm. 2011, 8(5), 1919-28. DOI: 10.1021/mp2002973.

32. Jensen, K.T.; Blaabjerg, L.I.; Lenz, E.; Bohr, A.; Grohganz, H.; Kleinebudde, P.; Rades, T.; Lobmann, K. Preparation and characterization of spray-dried co-amorphous drug-amino acid salts. J Pharm Pharmacol. 2016, 68(5), 615-24. DOI: 10.1111/jphp.12458.

33. Craye, G.; Lobmann, K.; Grohganz, H.; Rades, T.; Laitinen, R. Characterization of amorphous and co-amorphous simvastatin formulations prepared by spray drying. Molecules. 2015, 20(12), 21532-48. DOI: 10.3390/molecules201219784.

34. Alhajj, N.; O'Reilly, N.J.; Cathcart, H. Development and characterization of a spray-dried inhalable ciprofloxacin-quercetin co-amorphous system. Int J Pharm. 2022, 618, 121657. DOI: 10.1016/j.ijpharm.2022.121657.

35. Feng, Y.; Li, B.; Yang, L.; Liu, Y. Co-amorphous delivery systems based on curcumin and hydroxycinnamic acids: Stabilization, solubilization, and controlled release. LWT. 2022, 170, 114091. DOI: 10.1016/j.lwt.2022.114091.

36. Ojarinta, R.; Heikkinen, A.T.; Sievanen, E.; Laitinen, R. Dissolution behavior of co-amorphous amino acid-indomethacin mixtures: The ability of amino acids to stabilize the supersaturated state of indomethacin. Eur J Pharm Biopharm. 2017, 112, 85-95. DOI: 10.1016/j.ejpb.2016.11.023.

37. Ali, A.; Abdelhaleem, M.; Ali, A.A.; Maghrabi, I.A. Clozapine-carboxylic acid plasticized co-amorphous dispersions: Preparation, characterization and solution stability evaluation. Acta Pharm. 2015, 65(2), 133-46. DOI: 10.1515/acph-2015-0014.

38. Nair, A.; Varma, R.; Gourishetti, K.; Bhat, K.; Dengale, S. Influence of preparation methods on physicochemical and pharmacokinetic properties of co-amorphous formulations: The case of co-amorphous atorvastatin: Naringin. J Pharm Innov. 2020, 15, 365-79. DOI: 10.1007/s12247-019-09381-9.

39. Wu, W.; Lobmann, K.; Schnitzkewitz, J.; Knuhtsen, A.; Pedersen, D.S.; Grohganz, H.; Rades, T. Aspartame as a co-former in co-amorphous systems. Int J Pharm. 2018, 549(12), 380-87. DOI: 10.1016/j.ijpharm.2018.07.063.

40. Holzapfel, K.; Rades, T.; Leopold, C.S. CO-amorphous systems consisting of indomethacin and the chiral co-former tryptophan: Solid-state properties and molecular mobilities. Int J Pharm. 2023, 636, 122840. DOI: 10.1016/j.ijpharm.2023.122840.

41. Wairkar, S.; Gaud, R. Co-amorphous combination of nateglinide-metformin hydrochloride for dissolution enhancement. AAPS PharmSciTech. 2016, 17(3), 673-81. DOI: 10.1208/s12249-015-0371-4.

42. Bhalekar, M.R.; Madgulkar, A.R.; Desale, P.S.; Marium, G. Formulation of piperine solid lipid nanoparticles (SLN) for treatment of rheumatoid arthritis. Drug Dev Ind Pharm. 2017, 43(6), 1003-10. DOI: 10.1080/03639045.2017.1291666.

43. Anand, V.K.; Sakhare, S.D.; Sree, K.N.; Nair, A.R.; Varma, K.R.; Gourishetti, K. Dengale, S.J. The relevance of co-amorphous formulations to develop supersaturated dosage forms: In-vitro, and ex-vivo investigation of Ritonavir-Lopinavir co-amorphous materials. Eur J Pharm Sci. 2018, 123, 124-34. DOI; 10.1016/j.ejps.2018.07.046.

44. Shi, X.; Zhou, X.; Shen, S.; Chen, Q.; Song, S.; Gu, C.; Wang, C. Improved in vitro and in vivo properties of telmisartan in the co-amorphous system with hydrochlorothiazide: A potential drug-drug interaction mechanism prediction. Eur J Pharm Sci. 2021, 161, 105773. DOI: 10.1016/j.ejps.2021.105773.

45. Karagianni, A.; Kachrimanis, K.; Nikolakakis, I. Co-amorphous solid dispersions for solubility and absorption imrpovemnet of drugs: Composition, preparation, characterization and formulations for oral delivery. Pharmaceutics. 2018, 10(3), 98. DOI: 10.3390/pharmaceutics10030098.

46. Indian Pharmacopoeia, 8th edition.; The Indian Pharmacopoeia Commission Vol II, Ghaziabad, 2018, pp. 498-1500.

47. Lachman, L.; Lieberman, H. The theory and practice of Industrial Pharmacy, 3rd edition.; Varghese Publishing House, India, 1991, pp. 293-355.

48. Van krevelen, D.W.; Te Nijenhuis, K. Properties of polymers: their correlation with chemical structure; their numerical estimation and prediction from additive group contributions, 3rd edition.; Elsevier Science, Netherlands, 2008, pp. 129-87.

49. Favre, E.; Nguyen, Q.T.; Clement, R.; Neel, J. Application of Flory-Huggins theory to ternary polymer-solvents equilibria: A case study. Eur Polym J. 1996, 32(3), 303-09. DOI: 10.1016/0014-3057(95)00146-8.

50. Aryanti, P.P.; Ariono, D.; Hakim, A.N.; Wenten, I.G. Flory-Huggins based model to determine thermodynamic property of polymeric membrane solution. J Phys Conf Ser. 2018, 1090(1), 012074.

51. Wang, Z.; Sun, M.; Liu, T.; Gao, Z.; Ye, Q.; Tan, X.; Hou, Y.; Sun, J.; Wang, D.; He, Z. Co-amorphous solid dispersion systems of lacidipine-spironolactone with improved dissolution rate and enhanced physical stability. Asian J Pharm Sci. 2019, 14(1), 95-103. DOI: 10.1016/j.ajps.2018.11.001.

52. Garbiec, E.; Rosiak, N.; Zalewski, P.; Tajber, L.; Cielecka-Piontek, J. Genistein co-amorphous systems with amino acids: An investigation into enhanced solubility and biological activity. Pharmaceutics. 2023, 15(12), 2653. DOI: 10.3390/pharmaceutics15122653.

53. Aragon-Avurto, S.O.; Mondragon-Vasquez, K.; Valerio-Alfaro, G.; Dominguez-Chavez, J.G. Characterization, stability and solubility of co-amorphous systems of glibenclamide and L-arginine at different pH. Trop J Pharm Res. 2022, 21(7), 1355-64. DOI: 10.4314/tjpr.v2li7.1.

54. Lien, N.K.; Friscic, T.; Dar, G.M.; Gladden, L.F.; Jones, W. Terahertz time-domain spectroscopy and the quantitative monitoring of mechanochemical cocrystal formation. Nat Mater. 2007, 6(3), 206-9. DOI: 10.1038/nmat1848.

55. Laitinen, R.; Lobmann, K.; Grohganz, H.; Priemel, P.; Strachan, C.J.; Rades, T. Supersaturating drug delivery systems: The potential of co-amorphous drug formulations. Int J Pharm. 2017, 532(1), 1-12. DOI: 10.1016/j.ijpharm.2017.08.123.

56. Mendes, C.; Valentini, G.; Chamorro Rengifo, A.F.; Pinto, J.M.; Silva, M.S. Parize, A.L. Supersaturating drug delivery system of fixed drug combination: sulfamethoxazole and trimethoprim. Expert Rev Anti Infect Ther. 2019, 17(10), 841-50. DOI: 10.1080/14787210.2019.1675508.

57. Shi, N.Q.; Wang, S.R.; Zhang, Y.; Huo, J.S.; Wang, L.N.; Cai, J.H.; Li, Z.Q.; Ziang, B.; Qi, X.R. Hot melt extrusion technology for improved dissolution, solubility and “spring-parachute” processes of amorphous self-micellizing solid dispersions containing BCS II drugs indomethacin and fenofibrate: Profiles and mechanisms. Eur J Pharm Sci. 2019, 130, 78-90. DOI: 10.1016/j.ejps.2019.01.019.

58. Shi, N.Q.; Zhang, Y.; Li, Y.; Lai, H.W.; Xiao, X.; Feng, B.; Qi, X.R. Self-micellizing solid dispersions enhance the properties and therapeutic potential of fenofibrate: Advantages, profiles and mechanisms. Int J Pharm. 2017, 528(1-2), 563-77. DOI: 10.1016/j.ijpharm.2017.06.017.

59. Shi, Q.; Moinuddin, S.M.; Cai, T. Advances in coamorphous drug delivery systems. Acta Pharm Sin B. 2019, 9(1), 19-35. DOI: 10.1016/j.apsb.2018.08.002.

60. Kissi, E.O.; Khorami, K.; Rades, T. Determination of stable co-amorphous drug-drug ratios from the eutectic behavior of crystalline physical mixtures. Pharmaceutics. 2019, 11(12), 628.

61. Penzel, E.; Rieger, J.; Schneider, H.A. The glass transition temperature of random copolymer: Experimental data and the Gordon-taylor equation. Polymer. 1997, 38(2), 325-37. DOI: 10.1016/S0032-3861(96)00521-6.

62. Moinuddin, S.M.; Ruan, S.; Huang, Y.; Gao, Q.; Shi, Q.; Cai, B.; Cai, T. Facile formation of co-amorphous atenolol and hydrochlorohiazide mixtures via cryogenic-milling: Enhanced physical stability, dissolution and pharmacokinetic profile. Int J Pharm. 2017, 532(1), 393-400. DOI: 10.1016/j.ijpharm.2017.09.020.

63. Hancock, B.C.; Shamblin, S.L. Molecular mobility of amorphous pharmaceuticals determined using differential scanning calorimetry. Thermochimica acta. 2001, 380(2), 95-107. DOI: 10.1016/S0040-6031(01)00663-3.

64. Lobmann, K.; Laitinen, R.; Grohganz, H.; Strachan, C.; Rades, T.; Gordon, K.C. A theoretical and spectroscopic study of co-amorphous naproxen and indomethacin. Int J Pharm. 2013, 453(1), 80-87. DOI: 10.1016/j.ijpharm.2012.05.016.

65. Vasanti M.; Preeti S. HPLC Estimation, Ex vivo Everted Sac Permeability and In Vivo Pharmacokinetic studies of Darunavir. J Chrom Sci. 2018, 56(4), 307-16. DOI: 10.1093/chromsci/bmx113.